DETAILED REPORT ON LIF MEASUREMENTS OF FRESCOS BY GIUSTO DE' MENABUOI IN THE PADUA BAPTISTERY

F. Colao, L. Caneve, L. Fiorani, R. Fantoni, Ramiro Dell'Erba, V. Fassina

AGENZIA NAZIONALE PER LE NUOVE TECNOLOGIE,
L'ENERGIA E LO SVILUPPO ECONOMICO SOSTENIBILE

ISSN/0393-3016

DETAILED REPORT ON LIF MEASUREMENTS OF FRESCOS BY GIUSTO DE' MENABUOI IN THE PADUA BAPTISTERY

F. COLAO, L. CANEVE, L. FIORANI

ENEA - Unità Tecnica Sviluppo di Applicazioni delle Radiazioni
Laboratorio Diagnostiche e Metrologia
Centro Ricerche Frascati, Roma

R. FANTONI

ENEA - Unità Tecnica Sviluppo di Applicazioni delle Radiazioni
Centro Ricerche Frascati, Roma

R. DELL'ERBA

ENEA - Unità Tecnica Tecnologie Avanzate per l'Energia e l'Industria
Laboratorio Robotica
Centro Ricerche Casaccia, Roma

V. FASSINA

Soprintendenza ai Beni Storici Artistici ed Etnoantropologici
per le Provincie di Venezia, Belluno, Padova e Treviso
Palazzo Soranzo Cappello, Fondamenta Rio Marin
Via Santa Croce, 770 - 30135 Venezia

RT/2012/9/ENEA

AGENZIA NAZIONALE PER LE NUOVE TECNOLOGIE,
L'ENERGIA E LO SVILUPPO ECONOMICO SOSTENIBILE

DETAILED REPORT ON LIF MEASUREMENTS OF FRESCOS BY GIUSTO DE' MENABUOI IN THE PADUA BAPTISTERY

F. COLAO, L. CANEVE, L. FIORANI

ENEA - Unità Tecnica Sviluppo di Applicazioni delle Radiazioni
Laboratorio Diagnostiche e Metrologia
Centro Ricerche Frascati, Roma

R. FANTONI

ENEA - Unità Tecnica Sviluppo di Applicazioni delle Radiazioni
Centro Ricerche Frascati, Roma

R. DELL'ERBA

ENEA - Unità Tecnica Tecnologie Avanzate per l'Energia e l'Industria
Laboratorio Robotica
Centro Ricerche Casaccia, Roma

V. FASSINA

Soprintendenza ai Beni Storici Artistici ed Etnoantropologici
per le Provincie di Venezia, Belluno, Padova e Treviso
Palazzo Soranzo Cappello, Fondamenta Rio Marin
Via Santa Croce, 770 - 30135 Venezia

RT/2012/9/ENEA

DETAILED REPORT ON LIF MEASUREMENTS OF FRESCOS BY GIUSTO DE' MENABUOI IN THE PADUA BAPTISTERY

F. COLAO, L. CANEVE, R. FANTONI, L. FIORANI, R. DELL'ERBA, V. FASSINA

Abstract
Laser–induced fluorescence (LIF) is a powerful remote and non invasive analysis technique that has been successfully applied to the real-time diagnosis of historical artworks. Hyperspectral images collection on fresco's and their false colors processing allowed to reveal features invisible to the naked eye and to obtain specific information on pigments composition and consolidants utilization, the latter also related to former restorations. This report presents the results obtained by ENEA LIF–scanning system during a field campaign conducted in June 2010 on fresco's by Giusto de' Menabuoi in the Padua Baptistery.

Key words: *Laser induced fluorescence, consolidants, paraloid, acrilic tesins, PCA)*

RAPPORTO DETTAGLIATO SULLE MISURE LIF DEGLI AFFRESCHI DI GIUSTO DE' MENABUOI NEL BATTISTERO DI PADOVA

Riassunto
La fluorescenza indotta da laser (LIF) è una tecnica potente di analisi remota non invasiva che è stata applicata con successo alla diagnostica in tempo reale su beni culturali storici. La raccolta di immagini iperspettrali mediante sistemi di scansione su affreschi e la loro successiva elaborazione in falsi colori ha permesso di osservare caratteristiche invisibili ad occhio nudo e di ottenere informazioni specifiche relative alla composizione di pigmenti e all'utilizzo di consolidanti, anche in connessione con precedenti azioni di restauro. In questo rapporto sono presentati i risultati ottenuti mediante il sistema LIF–scanning dell'ENEA durante una campagna condotta nel giugno 2010 sugli affreschi di Giusto de' Menabuoi nel Battistero di Padova.

Parole Chiave: Fluorescenza indotta da laser, consolidanti, paraloid, tesine acriliche, PCA

INDEX

DETAILED REPORT ON LIF MEASUREMENTS OF FRESCOS BY GIUSTO DE' MENABUOI IN THE PADUA BAPTISTERY

1. Introduction

Innovative non destructive technologies suitable to the characterization of historical surfaces are currently under development mostly to satisfy the needs of conservators. Among spectroscopic techniques appropriate to remote application, the Fluorescence Induced upon ultraviolet Laser excitation (LIF) is capable to supply valuable information: it allows indeed for identification of fluorophores groups relevant to different substances either present onto the surface due to bio-degradation and environmental pollution of forming the outermost layers, for instance pigment, binders and consolidants in the case of painted surfaces. In particular restores need a precise knowledge of surface materials once engaged in removing traces of former restorations.

The retrieval of information on specific materials in multilayerd surfaces, as in the case of fresco's, relies on the construction of laboratory data bases to be used in combination with projection operators and on the application of statistical tool to disentangle major contribution in each examined surface point.

LIF images, collected in the Padua Baptistery and processed in order to retrieve information on constituent materials, are here presented and discussed. The field campaign was carried on in June 2010 prior to the planning of successive restorations. To this aim the investigation was focused onto the recognition of consolidant and binders, with the support of an available data base and the development of statistical tools for main spectral bands identification.

The construction of Padua Baptistery, located on the right side of the cathedral (see appendix), started in XII century and was accomplished in 1281. Its fresco's are considered Giusto de' Menabuoi's

masterpiece. In the present study, within a contract signed with Soprintendenza ai Beni Storici Artistici ed Etnoantropologici per le province di Venezia, Belluno, Padova e Treviso, selected areas of the Paradise fresco on the central dome and of the Genesis on the tambour have been investigated means of the ENEA LIF scanning system. This prototype is designed for remote operation with a high speed hyperspectral images acquisition based on the use of a structured laser beam shaped as a light blade. All collected images are shown in this report. Preliminary results obtained on the identification and distribution of pigments and consolidants, as retrieved by statistical image processing, are here presented and discussed.

2. Experimental

2.1 The set-up

The LIF scanning system developed and patented [1] at the ENEA laboratory in Frascati is capable to collect hyperspectral fluorescence images scanning large areas for applications to cultural heritage surfaces (e.g. frescos, decorated facades etc.). A new compact set up has been built, and successively patented [2], aimed to increase the performances in terms of space resolution, time resolved capabilities and data acquisition speed. Major achievements have been reached by a critical review of the optical design and consequently of the detector utilized [3]:

- the point focalization mode has been changed into a line focalization by using a quartz cylindrical lens and a imaging spectrograph (Jobin-Yvon CP240);
- the linear array detector, responsible for the multichannel spectral resolution, has been replaced with a square ICCD sensor (ANDOR iStar DH734, pixel size 13 μm), mounted behind a slit parallel to the laser line footprint during the scanning.

This arrangement is characterized by having the spatial and spectral information on two mutually orthogonal directions imaged on the detector, with submillimetric spatial resolution and a spectral resolution better than 2 nm. Additionally it is possible to implement time resolved measurements on the nanosecond scale by gating the spectral detector.

The overall current system performances are horizontal resolution 640 pixel, 0.1 mrad angular resolution, minimum acquisition time per line 200 ms, field of view (FOV) aperture 5.7° (corresponding to a scanned line of 2.5 m at 25 m distance). With the latter optics an image of $1.5\times5 m^2$ is scanned in less than 2 minute at 25 m.

The compact arrangement of the experimental apparatus is shown in Figure 1. The Nd:YAG compact laser source could be operated at two different wavelength in the UV: 355 nm or 266 nm, a few mJ of output energy were produced in short pulses (10 ns) at 20 Hz.

The performances of the LIF scanner are designed to fully exploit the information contained in spectral signature characteristic for each chemical compound laying on the examined surface [4]. The detection of the emitted fluorescence radiation allows to identify different materials utilized, mostly desired in view of a planned restoration. Indeed this system reveals with high spatial resolution the occurrence of retouches, traces of former restorations and consolidants not otherwise reported in the documentation relevant to the artwork. The system has also the chance to identify extraneous materials onto the surface

(degraded substances, pollutant, waxes, and residuals of biological attack such as microalgae and fungi) [5].

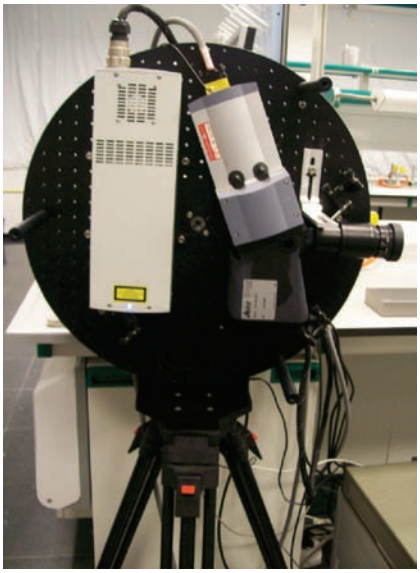

Figure 1 – Compact LIF line scanning, the vertical optical bench is mounted on a tripod, vertical scanning is performed by mean of an accurate stepping motor on the back side. Transmitting and receiving optics are in the front, the CCD and the laser on the rear.

2.2 Operating modes

The line scanning system can operate in two operating modes by slightly changing the active components in the entire device: i.e. reflectance and fluorescence measurements. These modes share indeed most of the optoelectronic equipment, namely the collection optics and the spectral detector, while differing, on one hand, in the way the sample is excited and, on the other hand, in the way the spectral detector is operated (see below the separate description).

Because of the use of refractive collecting optics, the focal planes for ultraviolet (UV) and visible (VIS) radiation occur in different position, causing defocus effects and degrading the spatial resolution. To overcome the related problems, successive separate acquisition runs are scheduled for every scan, each of them optimized for a specific wavelength range. The adoption of this measurement protocol results in a good detecting efficiency and high spatial resolution even in the very broad spectral range of radiation emitted upon laser excitation at 266 nm.

Actually, three consecutive acquisition runs are scheduled: in the first the collecting optics is focussed on the UV region from 250 to 450 nm; the successive two scans are focussed on the spectral region from 400 to 750 nm to acquire respectively the fluorescence induced in the visible and the reflectance image.

Reflectance measurements

Reflectance measurements are performed in a scan in which the laser is switched off while the sample is exposed to the light emitted by a NIST traceable lamp. The collection optics are focussed onto the scanned surface and the acquisition camera is running by locking its internal synchronism to the power line (to avoid image flickering). The result gives the reflectance spectrum for each pixel of the scanned

area, from which the CIE/lab coordinates can be computed once the system is calibrated against a reference surface.

Fluorescence measurements

The measurement of fluorescence spectra induced by laser is made by performing a scan while the laser light is on. The system uses a procedure to acquire spectra also in full day light: in this case a proprietary method is used to discriminate between the light induced from the laser (LIF signal) with respect to the light diffused by the area under study and by the environment. The result gives the fluorescence spectrum for each pixel of the scanned area; then a successive data analysis of the acquired spectrum provides detailed information on the area under study.

2.3 Analysis of spectral measurements

To speed up the processing of acquired images, the most relevant spectral features are identified by Principal Component (PC) analysis. Although it is commonly admitted that the PCs loadings do not possess any direct physical meaning, they can nevertheless be described in terms of bands. In some cases, a given PC loading has well defined spectroscopic bands with associated peaks, while in other cases more complicated trends and shapes are observed: most frequent is the case of a band set against another. Few of the PCs are usually retained for subsequent analysis: typically 5 to 8 components are enough to describe the entire spectral data set. It is also worth noticing the possibility to build suitable linear combinations of the computed PCs to have a faithful representation of each pixel spectra, eventually used for the computation of standard CIE/lab colorimetric measurements.

In the present report, the PC analysis is devoted to the identification of prominent spectral features, thus relieving from the lengthy time consuming examination of each acquired spectrum [6]. This procedure is advantageous because it is fast and can run in a semiautomatic mode. However, it has the inconvenience to give a global analysis, possibly ignoring those local peculiarities which do not possess enough statistical significance. To overcome this drawback local PC analyses are also performed on different portion of the scanned areas, then the results are analyzed separately. Once identified, spectral bands are sought for in the acquired LIF spectra, completing the data analysis.

A different method, used in the analysis of spectral images, concerns the identification of regions having a specific spectral content. Typical is the case of identification of a given pigment in an image: such task is accomplished either by a band analysis, or by using projection algorithms like SAM (Spectral Angle Mapper) or SCM (Spectral Correlation Mapper) in combination with an available data base [7]. Although the mapper algorithms perform well with a low computational cost, their performances are generally lower with respect to the band analysis procedures.

3. Results and discussion

3.1 Scans on Giusto de' Menabuoi's fresco's

In the Padua Baptistery several LIF scans were performed on frescos located in different positions, namely on the central dome (scans along East-West direction) and on the tambour. Details of the experimental conditions for the scans made on the vault are reported in Tables 1 to 6; the scans performed on the tambour are detailed in Tables 7 to 14; one additional portion of fresco (showing Canaan wedding) was examined on the north wall for calibration purpose; details are reported on Tables 15 and 16.

The LIF-scanning system was operated both in reflectance and fluorescence modes; the optical characterization of the scanned surfaces was completed with local complementary measurements: Raman spectra and spectrocolorimetric determinations of selected pigments were performed *in situ,* i.e. the surface was approached by means of an extensible mechanical arm.

Table 1 – Details of the preliminary scans IMG1 to IMG3

Scans	**IMG1**	**IMG2**	**IMG3**
Gate	500 ms	500 ms	500 ms
Gain	10	200	230
Laser current	OFF	OFF	OFF
Halogen lamp	1000 W	1000 W	1000 W
Optical f#	5.6	22	22
Spectral focus	VIS	VIS	VIS
Background			Y
Lines	600	600	100
Scan width	60000	60000	60000
Distance	15 m	15 m	15 m
Notes	Reflectance image	Reflectance image	Very low resolution reflectance image

Portion of the dome with delimitation of the scanned area. Real dimensions are approximately 1.5 m x 10 m; image size is 128 pixel width.

Table 2 – Details of the scans IMG4 to IMG7

Scans	IMG4_R	IMG5	IMG6	IMG7_R
Gate	500 ms	2000 ms	3000 ms	500 ms
Gain	230	250	250	250
Laser current	OFF	100 A	105 A	OFF
Halogen lamp	1000 W	OFF	OFF	1000 W
Optical f#	22	3.8	3.8	22
Spectral focus	VIS	UV	VIS	VIS
Background	Y			
Lines	600	600	600	600
Scan width	60000	60000	60000	60000
Distance	15 m	15 m	15 m	15 m
Notes	Reflectance image	LIF image	LIF image	Reflectance image

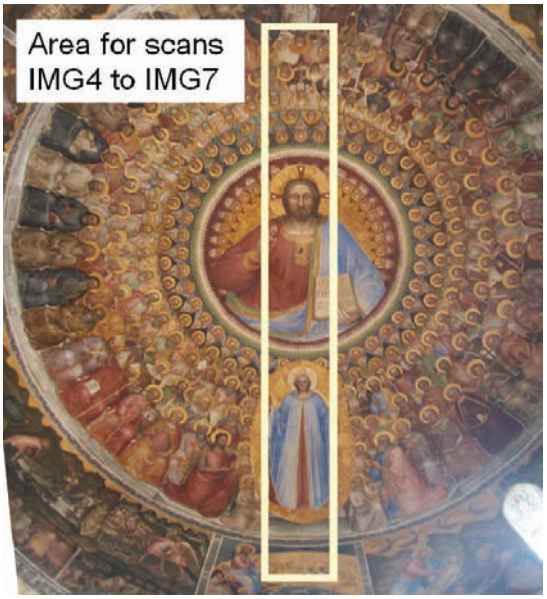

Portion of the dome with delimitation of the scanned area. Real dimensions are approximately 1.5 m × 10 m.

Table 3 – Details of the scans IMG8 to IMG10

Scans	IMG8_R	IMG9	IMG10
Gate	500 ms	3000 ms	3000 ms
Gain	250	250	250
Laser current	OFF	105 A	105 A
Halogen lamp	1000 W	OFF	OFF
Optical f#	22	3.8	3.8
Spectral focus	VIS	UV	UV/VIS
Background			
Lines	100	600	600
Scan width	60000	60000	60000
Distance	15 m	15 m	15 m
Notes	Reflectance image	LIF image	LIF image

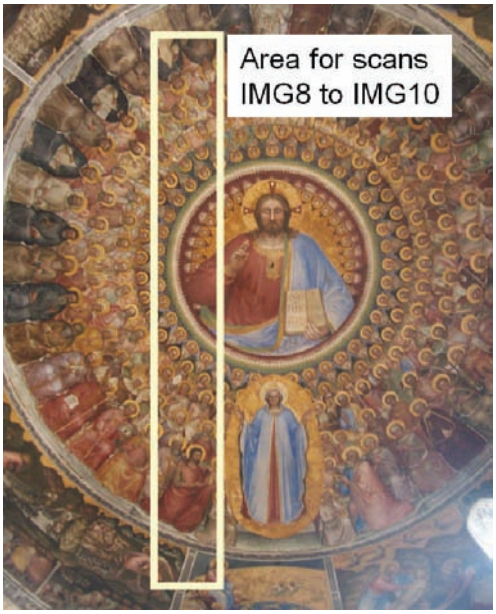

Portion of the dome with delimitation of the scanned area. Real dimensions are approximately 1.5 m × 10 m.

Table 4 – Details of the scans IMG11 to IMG13

Scans	IMG11	IMG12	IMG13_R
Gate	2000 ms	3000 ms	500 ms
Gain	250	250	250
Laser current	100 A	105 A	OFF
Halogen lamp	OFF	OFF	1000 W
Optical f#	3.8	3.8	22
Spectral focus	UV/VIS	UV	VIS
Background			
Lines	600	600	100
Scan width	60000	60000	60000
Distance	15 m	15 m	15 m
Notes	LIF image	LIF image	Reflectance image

Portion of the vault with delimitation of the scanned area. Real dimensions are approximately 1.5 m × 10 m.

Table 5 – Details of the scans T23 to T24

Scans	T23_UV	T24_R
Gate	5000 ms	600 ms
Gain	250	200
Laser current	105 A	OFF
Halogen lamp	OFF	1000 W
Optical f#	3.8	22
Spectral focus	UV	VIS
Background	Y	Y
Lines	2400	600
Scan width	60000	60000
Distance	20 m	18 m
Notes	LIF image	Reflectance image

Portion of the dome with delimitation of the scanned area. Real dimensions are approximately 1.5 m × 10 m.

Table 6 – Details of the scans T30 to T31

Scans	T30_R	T31_UV
Gate	1000 ms	4000 ms
Gain	250	250
Laser current	OFF	105A
Halogen lamp	1000 W	OFF
Optical f#	22	3.8
Spectral focus	VIS	UV
Background	Y	Y
Lines	600	600
Scan width	66000	66000
Distance	18 m	18 m
Notes	Reflectance image	LIF image

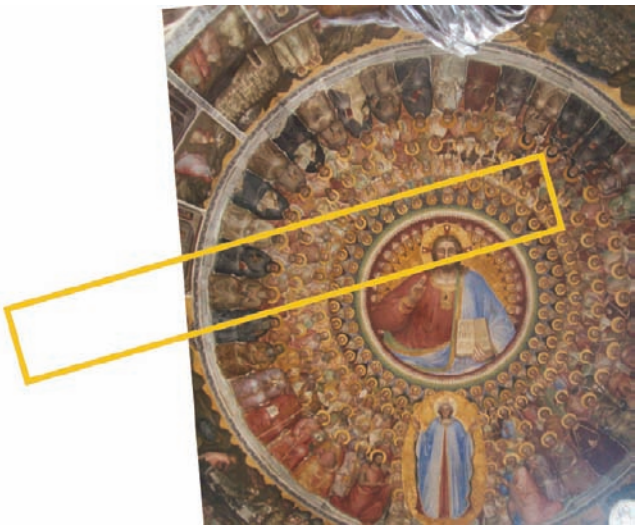

Portion of the dome with delimitation of the scanned area. Real dimensions are approximately 1.5 m ×10 m.

Table 7– Details of the scans IMG14 to IMG15

Scans	IMG14_R	IMG15
Gate	500 ms	3000 ms
Gain	250	250
Laser current	OFF	105 A
Halogen lamp	1000 W	OFF
Optical f#	22	3.8
Spectral focus	VIS	UV
Background		
Lines	300	400
Scan width	12000	12000
Distance	15 m	15 m
Notes	Reflectance image	LIF image

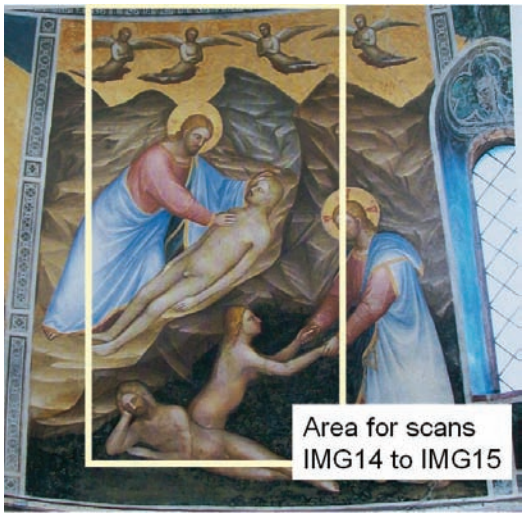

Portion of the tambour with delimitation of the scanned area. Real dimensions are approximately 1.5 m × 4 m; image size is 128 pixel width.

Table 8 –Details of the scans T10 to T13

Scans	T10_R	T11_R	T12_R	T13_R
Gate	100 ms	1000 ms	1000 ms	1000 ms
Gain	150	150	150	150
Laser current	OFF	OFF	OFF	OFF
Halogen lamp	1000 W	1000 W	1000 W	1000 W
Optical f#	22	22	22	22
Spectral focus	VIS	VIS	VIS	VIS
Background				
Lines	100	100	100	100
Scan width	12000	12000	12000	12000
Distance	18 m	18 m	18 m	18 m
Notes	Reflectance image	Reflectance image	Reflectance image	Reflectance image

Table 9 – Details of the scans T14 to T15

Scans	T14_R	T15_UV
Gate	1000 ms	5000 ms
Gain	150	250
Laser current	OFF	105 A
Halogen lamp	1000 W	OFF
Optical f#	22	3.8
Spectral focus	VIS	UV
Background		Y
Lines	100	100
Scan width	12000	14000
Distance	18 m	18 m
Notes	Reflectance image	LIF image

Portion of the frescoed tambour with delimitation of the scanned area. Real dimensions are approximately 1.5 m × 6 m.

Table 10 – Details of the scans T16 to T19

Scans	T16_UV	T17_R	T18_R	T19_UV
Gate	5000 ms	5000 ms	1000 ms	5000 ms
Gain	250	250	200	250
Laser current	105 A	OFF	OFF	105 A
Halogen lamp	OFF	1000 W	1000 W	OFF
Optical f#	3.8	3.8	22	22
Spectral focus	UV	VIS	VIS	UV
Background	Y	Y	Y	Y
Lines	150	150	150	150
Scan width	14000	14000	14000	14000
Distance	18m	18 m	18 m	18 m
Notes	LIF image	Reflectance image	Reflectance image	LIF image

Portion of the frescoed tambour with delimitation of the scanned area. Real dimensions are approximately 1.5 m × 6 m.

Table 11 – Details of the scans T20 to T22

Scans	T20_UV	T21_R	T22_UV
Gate	5000 ms	1000 ms	5000 ms
Gain	250	250	240
Laser current	105 A	OFF	105 A
Halogen lamp	OFF	1000W	OFF
Optical f#	22	22	3.8
Spectral focus	UV	VIS	UV
Background	Y	Y	Y
Lines	150	150	600
Scan width	14000	14000	14000
Distance	18 m	18 m	18 m
Notes	LIF image	Reflectance image	High resolution LIF image

Portion of the frescoed tambour with delimitation of the scanned area. Real dimensions are approximately 1.5 m × 8 m.

Table 12 – Details of the scans T32 to T36

Scans	T32_UV	T33_UV	T34_UV	T35_R	T36_R
Gate	4000 ms	4000 ms	4000 ms	4000 ms	4000 ms
Gain	250	250	250	250	250
Laser current	105 A	105 A	105 A	105 A	105 A
Halogen lamp	OFF	OFF	OFF	OFF	OFF
Optical f#	3.8	3.8	3.8	3.8	3.8
Spectral focus	UV	UV	UV	VIS	VIS
Background	Y	Y	Y	Y	Y
Lines	300	300	300	600	600
Scan width	66000	66000	66000	66000	66000
Distance	18 m	18 m	18 m	18 m	18 m
Notes	LIF image	LIF image (this is the repetition of T32 scan without spectrograph entrance slit)	LIF image	Reflectance image	Reflectance image

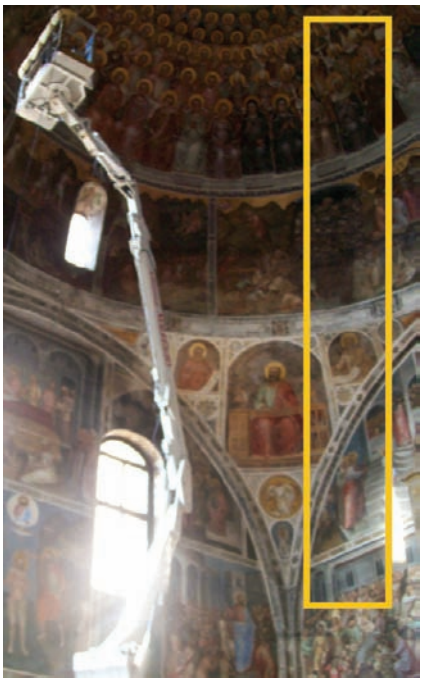

Portion of the frescoed tambour with delimitation of the scanned area. Real dimensions are approximately 1.5 m × 12 m.

Table 13 – Details of the scan A1

Scans	A1
Gate	1000 ms
Gain	N/A
Laser current	95% at 300 Hz
Halogen lamp	OFF
Optical f#	N/A
Spectral focus	UV
Background	Y
X pixels	140
Y pixels	106
Distance	1.5 m
Notes	LIF image with λ_{ex}=355nm

Portion of the frescoed tambour with delimitation of the scanned area. Real dimensions are approximately 1.2 m × 0.5 m.

Table 14 – Details of the scan A2.

Scans	A2
Gate	1000 ms
Gain	N/A
Laser current	95% at 300 Hz
Halogen lamp	OFF
Optical f#	N/A
Spectral focus	UV
Background	Y
X pixels	140
Y pixels	140
Distance	1.5 m
Notes	LIF image with λ_{ex}=355 nm

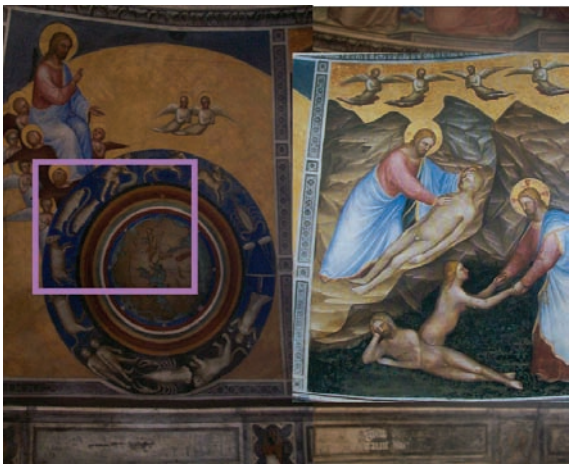

Portion of the frescoed tambour with delimitation of the scanned area. Real dimensions are approximately 1.1 m × 0.9 m.

Table 15 – Details of the scans P1 to P2.

Scans	P1	P2_R
Gate	3000 ms	500 ms
Gain	250	150
Laser current	105 A	OFF
Halogen lamp	OFF	Sun light
Optical f#	3.8	3.8
Spectral focus	UV	VIS
Background		
Lines	100	100
Scan width	15000	15000
Distance	8 m	8 m
Notes	LIF image	Reflectance image

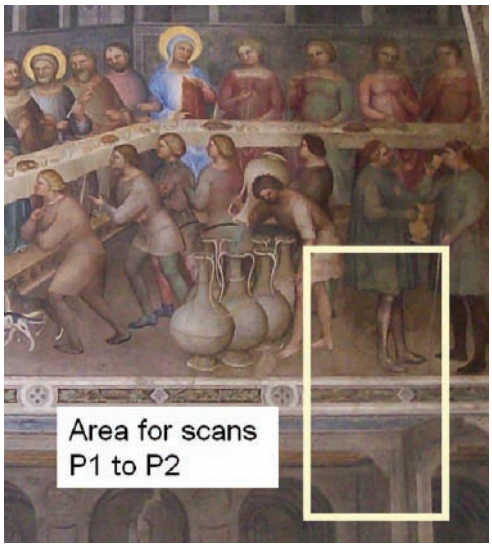

Portion of the Northern wall with delimitation of the scanned area. Real dimensions are approximately 1.5 m x 4 m; image size is 128 pixel width.

Table 16 – Details of the scans P3 to P4

Scans	P3_R	P4
Gate	500 ms	3000 ms
Gain	150	250
Laser current	OFF	105 A
Halogen lamp	Sun light	OFF
Optical f#	3.8	3.8
Spectral focus	VIS	UV
Background		
Lines	300	300
Scan width	18000	18000
Distance	8 m	8 m
Notes	Reflectance image	LIF image

Portion of the north wall with delimitation of the scanned area. Real dimensions are approximately 1.5 m × 5 m.

3.2 Scan on the dome

A portion of the dome was used for preliminary LIF measurements aimed at optimizing the system performances on frescos. The LIF camera was placed at a distance larger than 19 m from the surface and several images were acquired with a spatial resolution of approximately 0.015 m. The scan size was 128 pixels width, 100 to 2400 pixels height and 250 spectral channels from 200 nm to 800 nm; the nominal spectral resolution was 2.5 nm. Several optical and electronic system parameters (objective diaphragm aperture, exposure time, etc.) were optimized.

The details of the acquisition mode for the scans acquired on the dome are summarized in Tables 1 to 6.

Analysis of reflectance spectra

Figure 2 shows the RGB image obtained from the processing relative to the first three scans: in all scans

Figure 2 – a) RGB reconstruction from scan IMG2_R (reflectance image, 600 lines) with spectral channel at 600 nm, 500 nm, 400 nm ;b) RGB reconstruction of a very low resolution scan IMG3_R (reflectance image, 100 lines) with spectral channel at 600 nm, 50 0nm, 400 nm; c) RGB reconstruction from scan IMG4_R (reflectance image, 600 lines) with spectral channel at 600 nm, 500 nm, 400 nm.

the camera was operated for reflectance measurement. Right and left portions of Figure 2a,c show images acquired with high resolution, while the central panel (fig. 2b) is acquired with a reduced number of line scan. High resolution scans reveal plenty of details: indeed it is possible to recognize some of the letters on the book hold on the left hand of Our Lord. The reduction of the number of line scans causes a degradation of the image: however many features of the characters there represented are still recognizable. We conclude that also in case of very low resolution images, it is possible to discern the contours of several elements there represented, giving the possibility to precisely locate peculiar spectral features.

Relevant spectral features on the acquired images are identified by PC analysis. Figure 3 shows the PC loadings on image IMG2: here we observe that the first PC (PC1) is characterized by a smooth spectrum, very close to the average. The second PC (PC2) has two extrema at 490 nm (maximum) and 590 nm (minimum): their presence can be interpreted as a rough representation of independent characteristics. The third PC (PC3) has an oscillatory initial trend followed by an maximum at 700nm. It is worth noticing that the spectral intensity in the blue, green and red spectral regions can be obtained by a suitable linear combination of the first three components PC1, PC2 and PC3: although it is not possible to assign any of the PCs to the RGB colour components, a suitable linear combinations could give a result equivalent to the standard CIE/lab measurements, at least from a colorimetric point of view.

A close observation of the reflectance image in Figure 2a reveals an interesting feature just under the right hand of Our Lord: here we notice an area with a more saturated red colour. The spectral analysis shows the occurrence of an emission appearing as a spectral anomaly in the ratio of the spectral amplitudes at 620nm and 477nm, as shown in Figure 4. To spatially localize this features, we performed a pigment classification according to an automatic analysis based on the SAM algorithm. At first, in the absence of a complete data base with pigments on fresco [8,9], we do not have any reference, then an internal endpoint for the mapper is chosen by selecting a region in marked areas (see left side of Figure 4).

Figure 5 shows the result of SAM image processing: on Figure 5a an endpoint is selected to identify the regions coloured with the red pigment; in Figure 5b the reference endpoint used has also the observed spectral band at 400 nm; on Figure 5c an image processing based on a single band intensity analysis is shown.

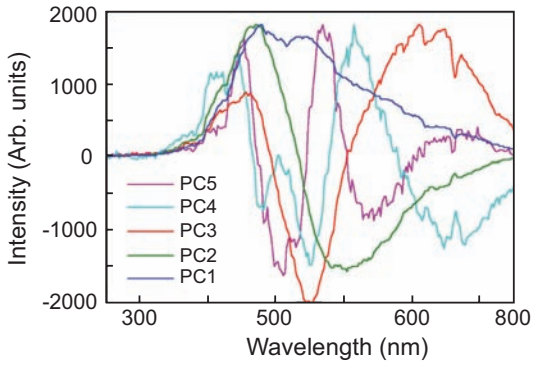

Figure 3 – PC analysis of image IMG2_R.

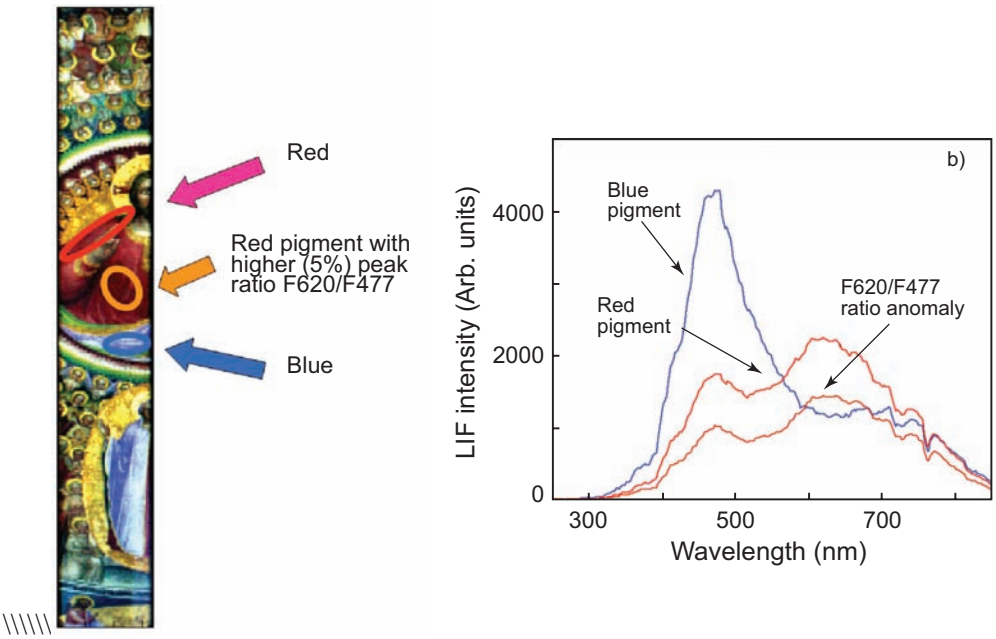

Figure 4 – Selection of pigments spectra in scan IMG2_R a) and the corresponding spectra b).

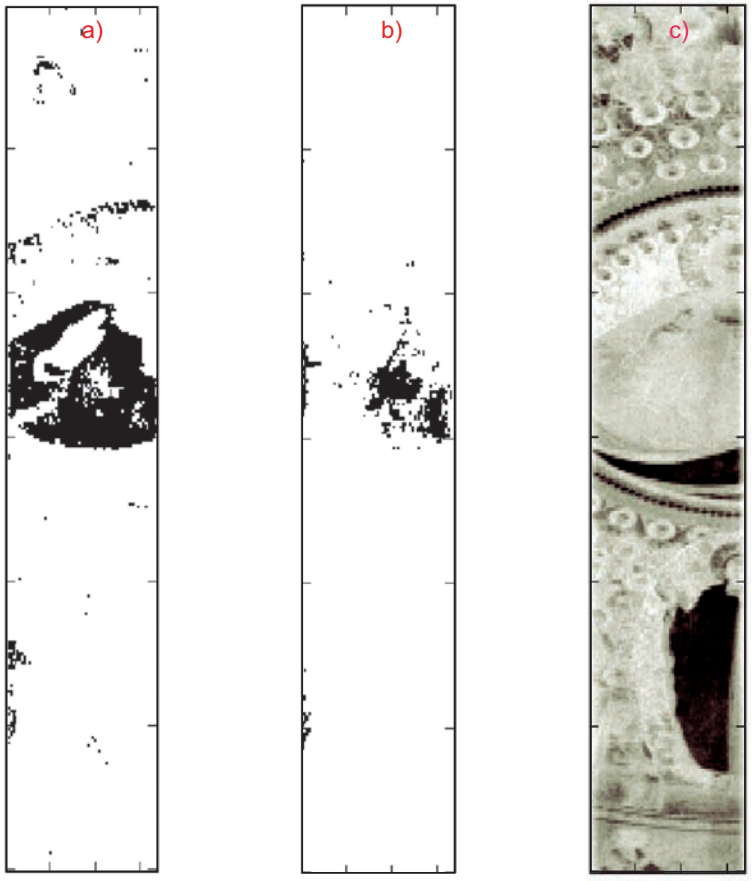

Figure 5 – The SAM was used in IMG2_R to identify areas dominated by specific spectral features: a) identification of red pigment; b) identification of pixels with bimodal spectrum; c) single band analysis at F400 nm.

We observe that SAM performs in an excellent way, since it recognize the entire area with the evidenced spectral anomaly, and, on the other hand, a single band analysis is not suitable for the identification of the observed spectral feature because of the strong spectral interference caused by the maximum around 450 nm in the blue-green fluorescent emission.

The presented experimental findings, demonstrate the ability to discriminate spectral differences in the peak ratio (F620/F477) of about 5% or even lower. The noticed spectral anomaly is precisely localized in Figure 5b, however its meaning is not yet completely clear. Several causes could contribute, possibly at the same time: presence of humidity in the wall, use of consolidants, presence of protecting varnishes and/or glossy superficial layers, retouches. Unfortunately, complementary information from Raman spectra could not be not be collected, thus it was not possible to discriminate among the different causes reaching a definite conclusion, nevertheless this is an area deserving attention and requiring study with complementary techniques (microstratigraphy, XRF, etc.).

Identification of bands in LIF spectra

The band identification in LIF spectra excited at 266 nm was preceded by PC Analysis. Figure 6 shows the PC components of images IMG5 (upper left side acquired with focus in the UV spectral region), IMG6 (upper right side acquired with focus in the VIS spectral region) and IMG9 (lower left side acquired with focus in the UV spectral region). As expected, the spectral content is different in the two upper plots, which refer to the same region. The largest difference concerns the spectral amplitude in the 500 nm region of PC1: the acquisition with focus in the UV is nearly zero, while the other with focus in the VIS still has a relevant contribution.

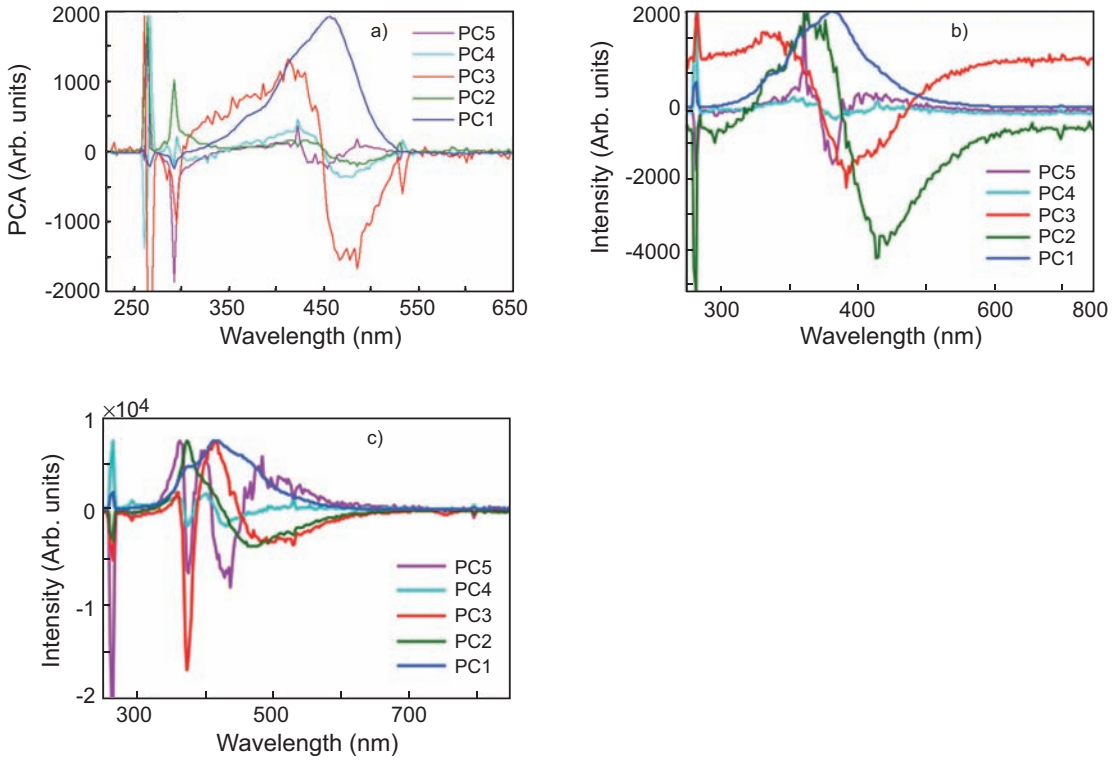

Figure 6 – PC analysis of LIF scan of IMG5 a), IMG6 b), IMG9 c).

The most interesting spectral features observed in Figure 6 are:

- the elastic backscatter at 266 nm is visible in all of the plot of Figure 6 (this wavelength is strongly attenuated then its amplitude is not driving to saturation the detector);
- a strong narrowband emission peaked at 293 nm (FWHM 8 nm), corresponding either to a narrow UV fluorescence band or to Raman shift of 3460 cm^{-1};
- a broadband emission in the region 400-500 nm;
- smaller intensity bands in UV around 350 nm (Fig. 6a) and 500 nm (Fig. 6b);
- a relatively narrow band peaked at 370 nm (FWHM 20 nm) (Fig. 6c);

Although it is of uttermost importance to assign each of these bands to specific pigments, binders and consolidants, the exact determination of the nature of the compound from which the LIF spectrum originates is not easy. Our analysis will then proceed first by looking to their occurrence in the acquired scans, successively an interpretation is attempted based on our previous experiences by comparison with a reference spectral data base available for a limited number of consolidants [5,6].

A first qualitative result from LIF scans is obtained by combining three different bands into one RGB coloured image; the application of this data processing allows to get the false colour images presented in Figures 7 to 11. Figure 7a shows the RGB representation of scan IMG5 with the RG bands at 420 nm

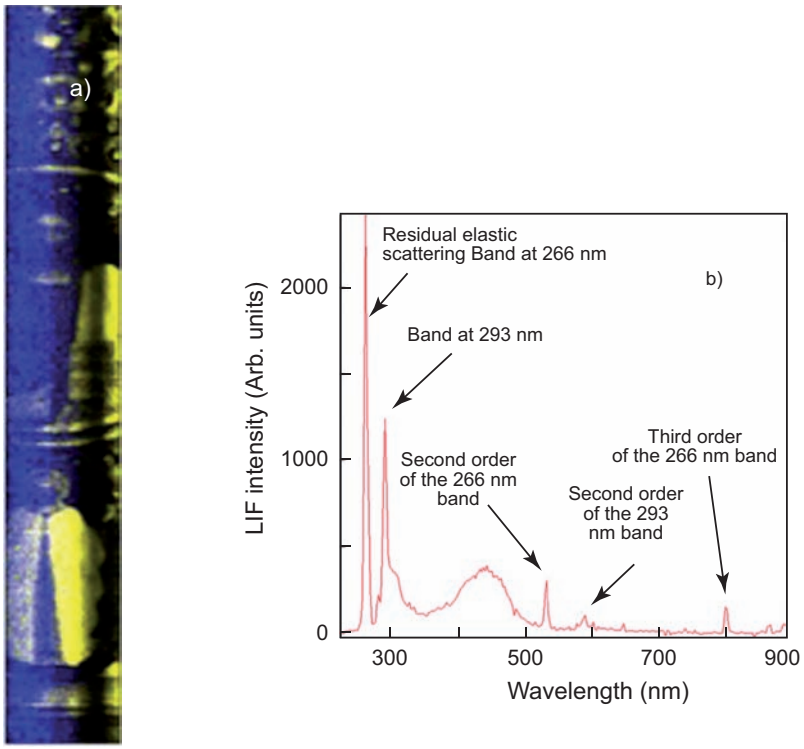

Figure 7 – a) RGB false colour reconstruction from image IMG5 with the RG bands at 420 nm and the B band at 293 nm; b) average spectrum of scan IMG5: note the prominent emission at 293 nm resulting in a blue colour most on the left side; the non uniform appearance of the emission is due to an incomplete correction of spatial equalization.

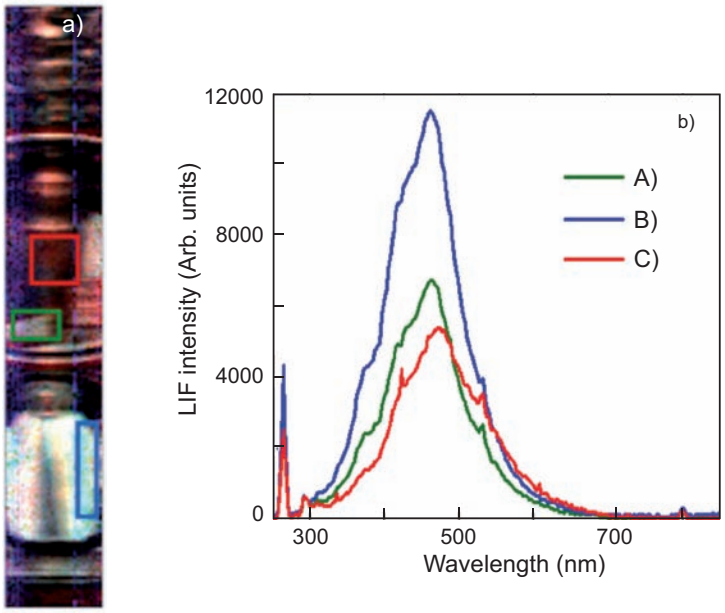

Figure 8 – a) RGB false colour reconstruction from image IMG6 with bands at 331nm, 400 nm.

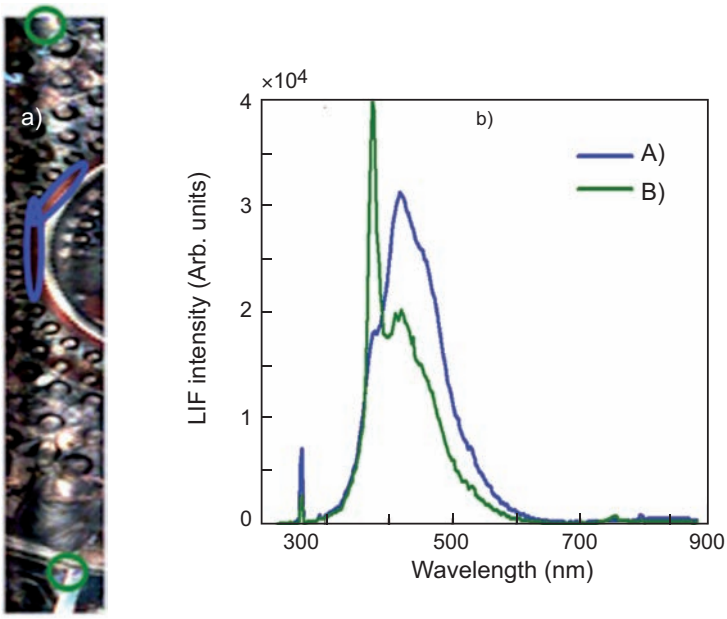

Figure 9 – a) RGB false colour reconstruction from image IMG9 with bands at 331nm, 400 nm and 550 nm; b) average spectra in selected regions: a prominent band at 375 nm is found on some points evidenced by elliptical marks in the left side.

and Figure 7b band at 293 nm while Figure 8a represent the false colour image of scan IMG6 with bands at 331 nm, 400 nm and 550 nm. Figures 9 and 10 show respectively the RGB reconstruction of scans IMG9 and IMG11.

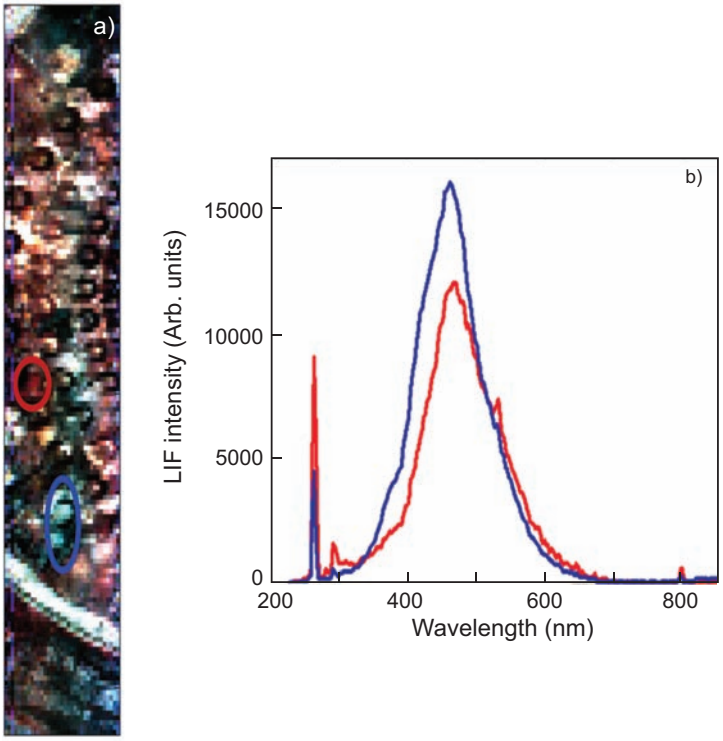

Figure 10 – a) RGB false colour reconstruction from image IMG11 with bands at 331 nm, 400 nm and 550 nm; b) average spectra in selected regions: a prominent band at 293 and at 373 nm is found on some points. The plot on right side shows the corresponding LIF spectra.

The plot Figures 7b to 10b shows some of the spectra from areas with an identified peculiar spectral content. As a general observation, we note in all spectra here reported, see for example Figure 7b, two clearly discernible weak features around 532 nm and 798 nm: actually they are an artefact of the spectrometer corresponding to the second and third diffraction order of the strong backscattered laser emission at 266 nm. Similarly the spectral structure at 586 nm is the second diffraction order of the intense band at 293 nm.

LIF emissions are also observed: it is worth mentioning the prominent band around 370 nm (see Fig. 9b), which is tentatively assigned to PARALOID B72. Induced emissions at 311 nm, and 370 nm are visible also in Figures 8b, 10b and 11b.

Based on the results of PC analysis, some interesting spectral features are extracted by the careful examination of single pixel LIF spectra. To this purpose we plot the image of band intensity at 293 nm: Figure 12a shows that absolute LIF intensity at 293 nm is approximately the same in different region of the image. By assuming a monotonic relationship between peak intensity and the amount of the chromophore originating the signal (eventually a linear relationship is assumed) we infer a nearly uniform distribution of the constituent responsible for the observed strong emission.

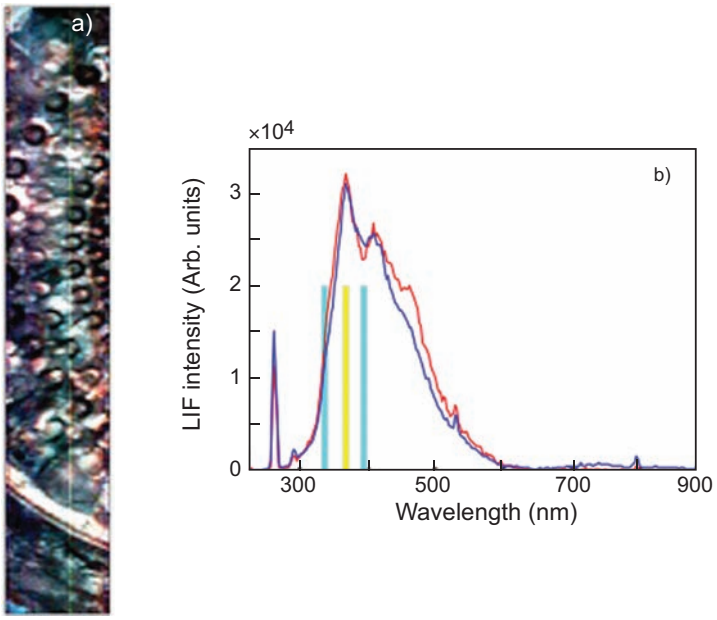

Figure 11 – a) RGB false colour reconstruction from image IMG12 with bands at 331 nm, 370 nm and 450 nm; b) average spectra in selected regions: the band at 293 is easily found just on the right of the elastic backscattering, while that at 373 nm is prominent in almost all the scanned area.

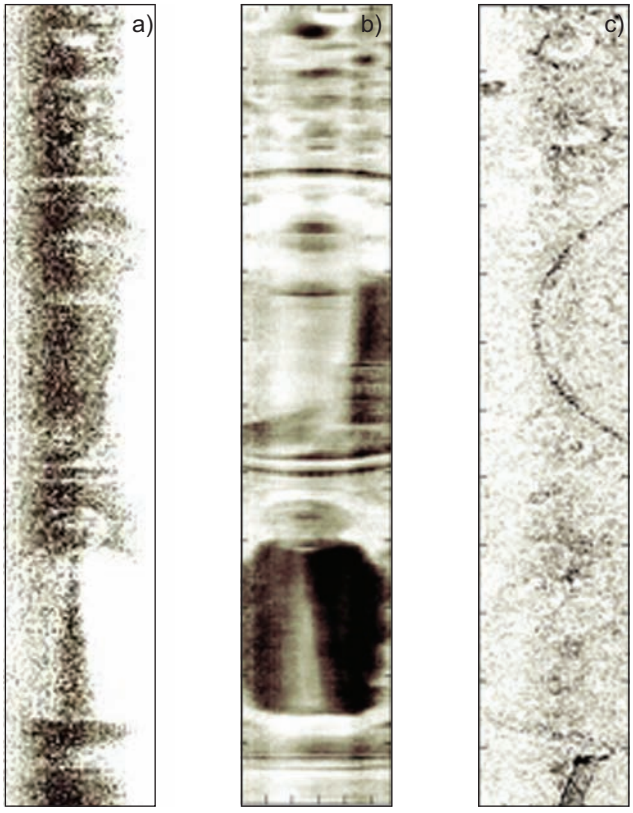

Figure 12 – a) Band analysis of the F293 nm peak in IMG5 scan; b) band analysis of the F480 nm peak in IMG6 scan; c) band analysis of the F377 nm peak in IMG9 scan; grey levels are used to indicate the fluorescence intensity (dark grey to black corresponds to higher LIF intensity).

The substance responsible for the emission at 293 nm spatially localized in Figure 12a can range among several candidates, eventually contributing and interfering at the same time. Nearly uniform distribution is also observed in IMG9 scan, thus supporting for the hypothesis of a widespread use of the associated chemical, probably an organic polymer used as consolidant, in all the scanned areas.

Several chemicals are compatible with the observed spectral feature; among the substances commonly used, we must include glossy varnishes and/or consolidants like PRIMAL AC33 (acrylic resin) MOVILITH (polyvinyl acetate); even water (in form of high humidity and/or water droplets over the painted layer) is compatible with the observed spectrum, provided that the emission is ascribed to a Raman shift (O-H stretching around 3460 cm^{-1}), however the water Raman band is not very intense and a quite thick layer should be present to generate such a well defined spectral feature. A more precise identification and a discrimination between various substances is not possible because Raman spectra on this region could not be collected by the available instrumentation (limited to Raman shift below 2200 cm^{-1}). For a complete identification we recommend further analysis of the surface in the areas located in Figure 11a with complementary technique (microstratigraphy, XRF, micro-diffractometry, etc.).

A detailed analysis of scans IMG5 and IMG6 is presented in Figure 13: here different algorithms are run to precisely localize the place of emission of the band peaked at 375nm and attributed to PARALOID B72. Figure 13a shows the results obtained by applying the SAM algorithm; in this case, as reference spectrum we use an internal endpoint on pixels having a large peak amplitude at 375 nm. The entire Figure 13a shows a scattered distribution with a hot spot in the lower right part. This analysis

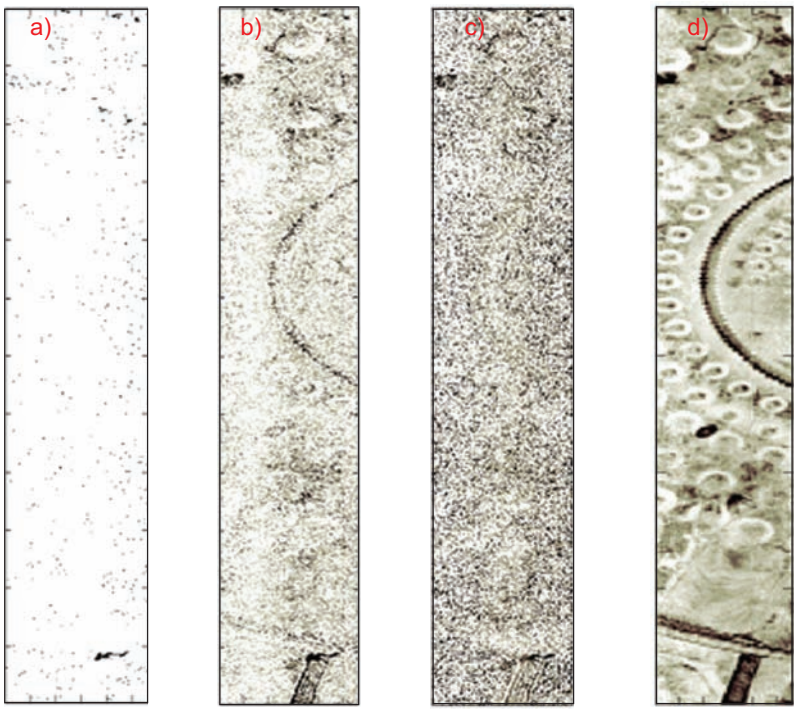

Figure 13 – a) SAM similarity map for identification of areas with a prominent fluorescent emission at 375 nm; b) band analysis: absolute band intensity F360; c) band ratio analysis: F375 is normalized to F450, dark grey levels corresponds to high band ratio values; d) F377 band analysis: the background at B337 and B383 is subtracted from the fluorescence; the image is also corrected for spatial change in detecting efficiency (spatial equalization).

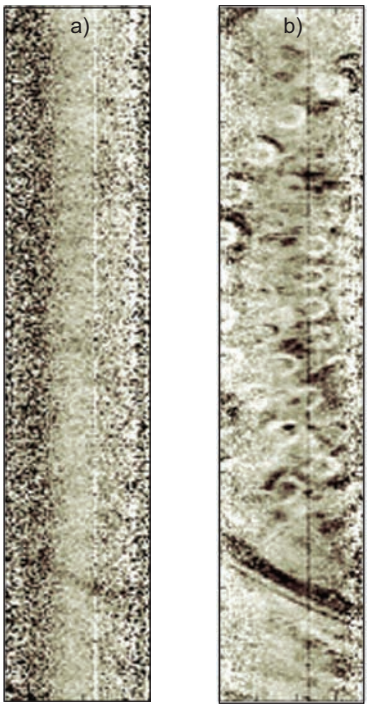

Figure 14 – A) Band analysis at F293 for identification of areas with a prominent emission at 293nm, in IMG12 (background was taken at 280nm and 308nm respectively); B) band analysis at F369 for identification of areas with a prominent emission at 369nm, in IMG12 (background was taken at 339 nm and 395nm respectively), dark grey levels corresponds to high band ratio values.

is completed with a band analysis at 360 nm. The result is shown in Figure13b, where we can better localize the maximum intensity of the emission. A similar result is shown in Figure13c.

The most interesting result is finally obtained by a band analysis made by correcting the fluorescence band for the contribution coming from the background (at 337 nm and 383 nm). The result is shown in Figure 13d, where we observe some hot spot hidden to the previous analyses and now appearing around at half of the image as a black spot.

Similar results have been obtained also for the scan of IMG12; Figure 14a shows the band analysis for the peak at 293 nm, while Figure 14b reports the band analysis of the peak at 370 nm.

3.3 Scan of the tambour

Several regions in the *tambour* were scanned by the LIF apparatus; most of the scans were made with excitation at 266 nm, while few others were made with excitation at 355 nm. The LIF camera was placed at more than 18 m distance from the target and several images were acquired with a spatial resolution of approximately 0.012 m. Details of the acquisition mode for the scans acquired on the *tambour* are summarized in Tables 7 to 14.

Analysis of reflectance spectra

Reflectance spectra were recorded only from regions scanned also by the deep UV excitation LIF system. Figure 15 reports the area of the scans IMG14 and IMG15: the left part show a conventional photograph, while the right part show the RGB reconstruction obtained by a low resolution reflectance

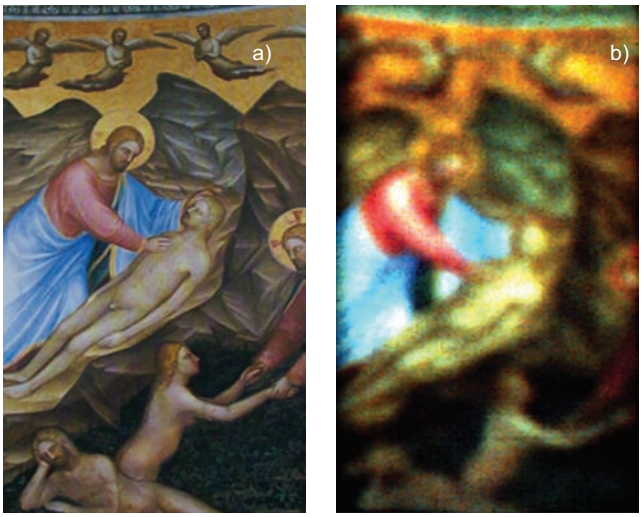

Figure 15 – a) Conventional photo of the area analyzed by scans IMG14 and IMG15; b) low resolution RGB image from scan IMG14_R (reflectance image) with spectral channels at 600 nm, 500 nm, 400 nm.

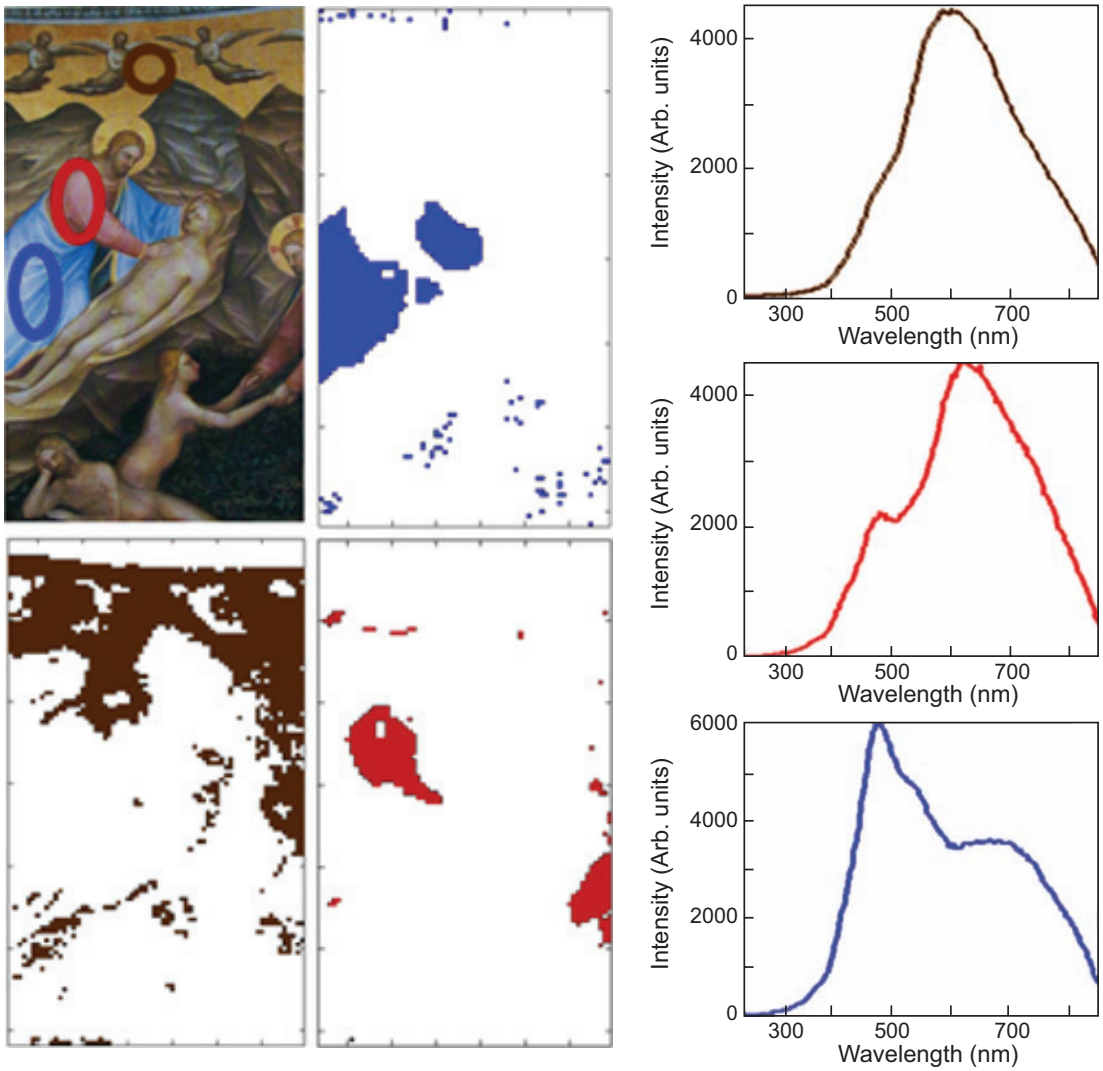

Figure 16 – Pigments identification in scan IMG14_R and the corresponding spectra.

scan. The acquired reflectance images are then used to recognize the spatial distribution of the pigments.

Figure 16 shows the result of SAM image processing: three different endpoints are selected to identify the regions colored with the red, blue and light brown pigment. We observe the excellent performance of SAM, able to precisely identify areas with the selected pigment spectra.

Identification of bands in LIF spectra

The identification of band in LIF spectra was preceded by a PC analysis. Figure 17 shows the PC components of images IMG15, P4, T19 and T23: all were acquired with the focus in the UV spectral region. The spectral content is similar to that presented in Figure 7b, however a couple of spectral features are now more prominent: namely the bands peaked at 310 nm and 338 nm; in Figure 17a the peak at 293 nm is well distinguishable, as also the peak at 375 nm. The latter is even more evident in Figure 17b; both peaks also appear in some of the PC in Figure 17c and d. While recalling the lack of physical meaning in PC components, we stress their use as hint to analyze the physical LIF spectra.

As an application of the output obtained by the use of this procedure, the search for peculiar spectral features in the scan of IMG15 is performed. The results of Figure 18 shows the identification of small regions or even pixels having a LIF spectra with peaks at 293 nm, 313 nm and 375 nm.

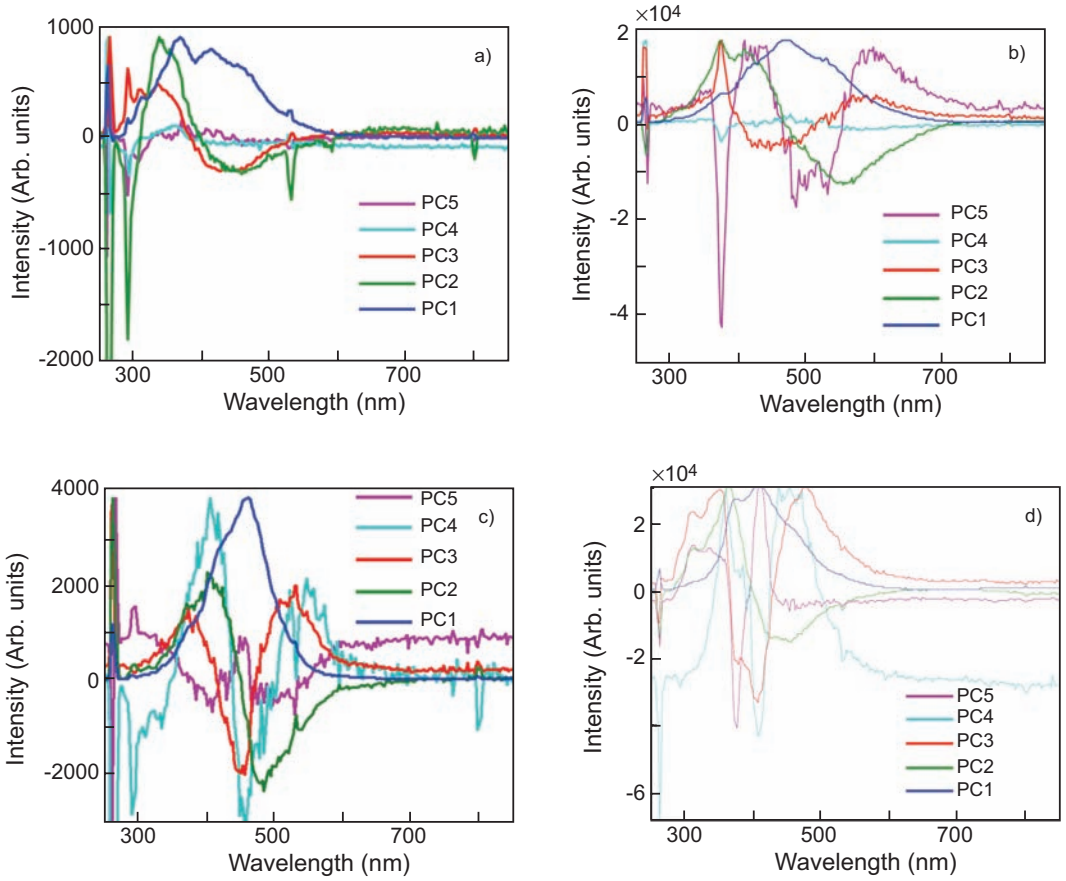

Figure 17 – a) PC analysis of LIF scan of IMG15; b) PC analysis of LIF scan of P4; c) PC analysis of LIF scan of T19; d) PC analysis of LIF scan of T23

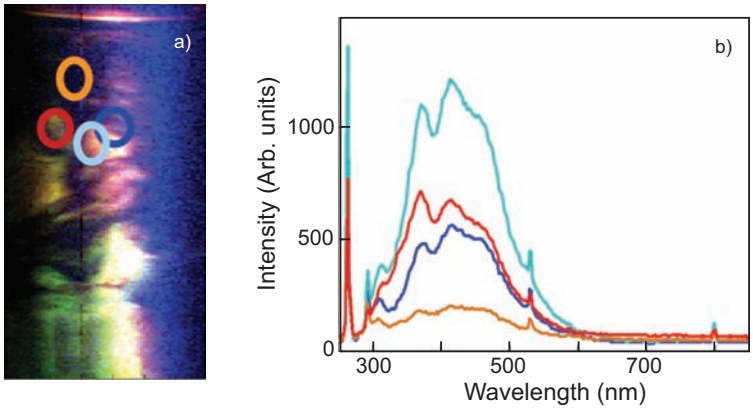

Figure 18 – a) RGB reconstruction from data of scan IMG15 using spectral channels at 293 nm, 313 nm and 375 nm, b) LIF spectra on selected areas shown on the right side.

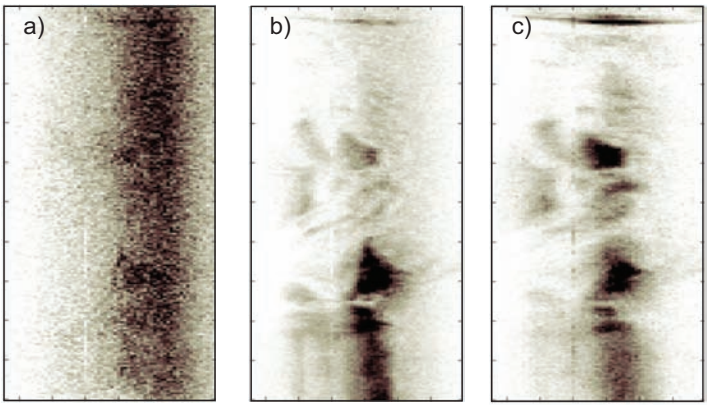

Figure 19 – Selected LIF images from scan IMG15: a) F293 band with background at 287 nm and 298 nm, b) F313 band with background at 303 nm and 323 nm, c) F375 band with background at 354 nm and 390 nm.

To spatially localize areas with the mentioned spectral features we report in Figure 19 the LIF intensity emissions at 293 nm, 313 nm and at 375 nm coded in a grey scale; here the focus is put on a single band and the resulting output is an image with 64 levels. Data represented in Figure 19 can be used as a qualitative and semiquantitative measurements of the amount of substance responsible for the observed spectral emission.

As an example, let us take into account the emission at 375 nm (PARALOID): the data reported in Figure 19b do constitute a qualitative measurement of the amount of such chemical on the scanned surface. Nevertheless, a calibration is mandatory whenever an accurate quantitative measurement is needed. Although the calibration of spectral data it is still possible, it is presently out of the scope of the present work.

The result of the analysis made on scan P4 (taken on a portion of the wall) is shown in Figure 20. In the left part it is reported the RBG reconstruction with LIF emission intensity at 375 nm, 500 nm and 600 nm: here we notice an area dominated by a bluish colour, having the meaning of high intensity at 375 nm (PARALOID B75); the spectrum is shown in Figure 20b while the qualitative measurement of chemical amount on the surface is shown in Figure 20c of the same figure.

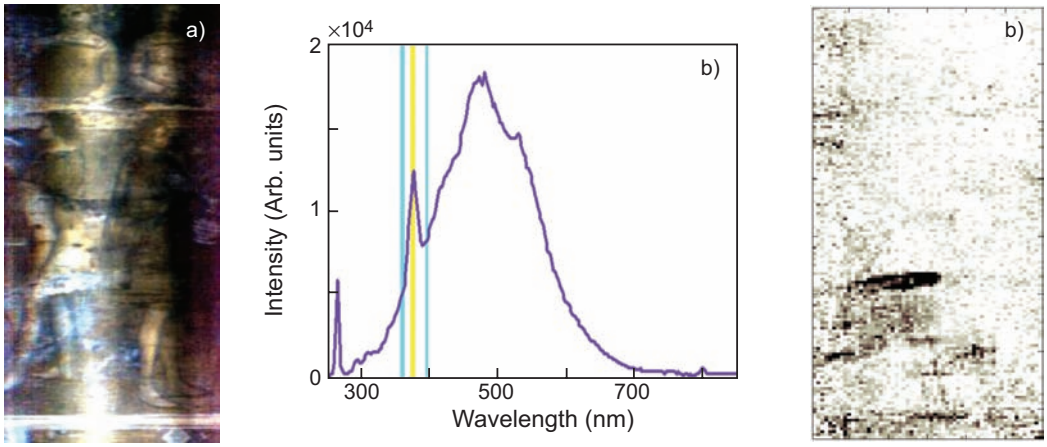

Figure 20 – Band analysis of scan P4: a) RGB false colour reconstruction (R600, G500, B375); b) LIF spectrum of the bluish dominated areas (close to the right leg of the servant;) c) grey level scale of the intensity at F375 band with background at 354 nm and 390 nm.

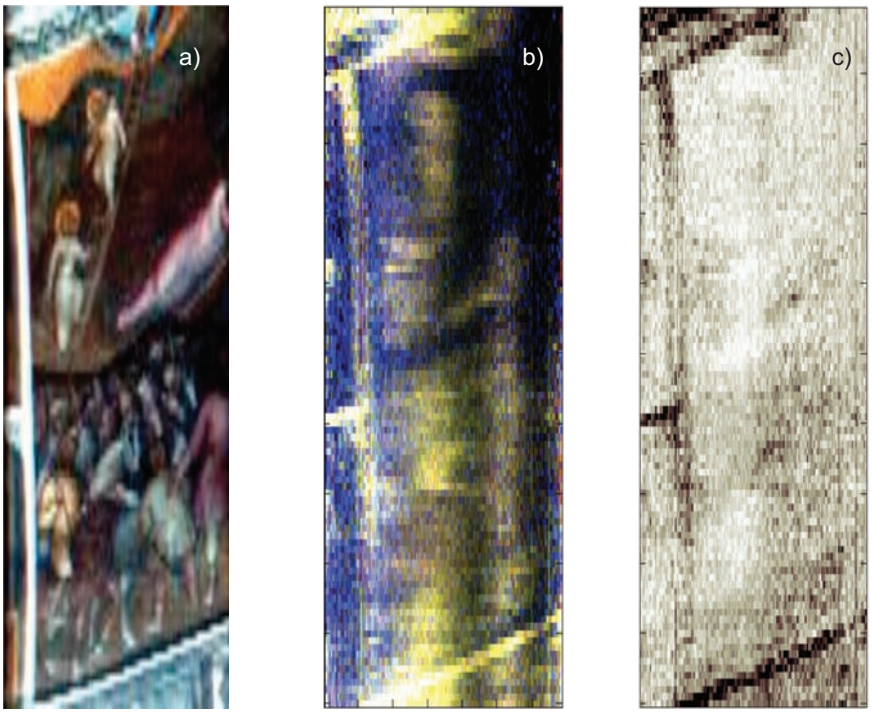

Figure 21 – Band analysis of scan T14 and T15: a) RGB colour image from spectrocolorimetric data; b) false colour reconstruction (RG420, B293); c) grey level scale of the intensity at F375 band with background at 354 nm and 390 nm.

Similar experimental findings are also obtained for scans performed on different portion of the *tambour*: the results are shown in Figures 21 to 23; in part a) of these figures it is reported the RGB image for the purpose of spatial localization; part b) of the same figures shows the LIF emission intensity of two channels combined to obtain a two colour reconstruction (RG at 420 nm and B at 375 nm); in part c) the qualitative measurement of the chemical compound layered on the surface is obtained from the fluorescence band intensity at 370 nm (PARALOID).

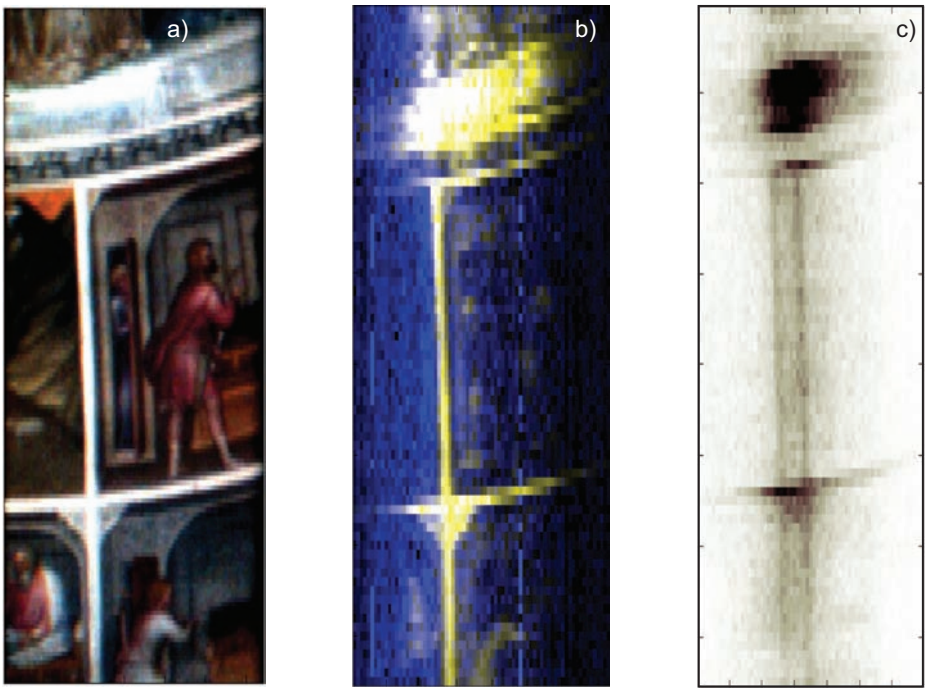

Figure 22 – Band analysis of scan T16 to T19: a) RGB colour image from spectrocolorimetric data; b) false colour reconstruction (RG420, B293); c) grey level scale of the intensity at F375 band with background at 354 nm and 390 nm.

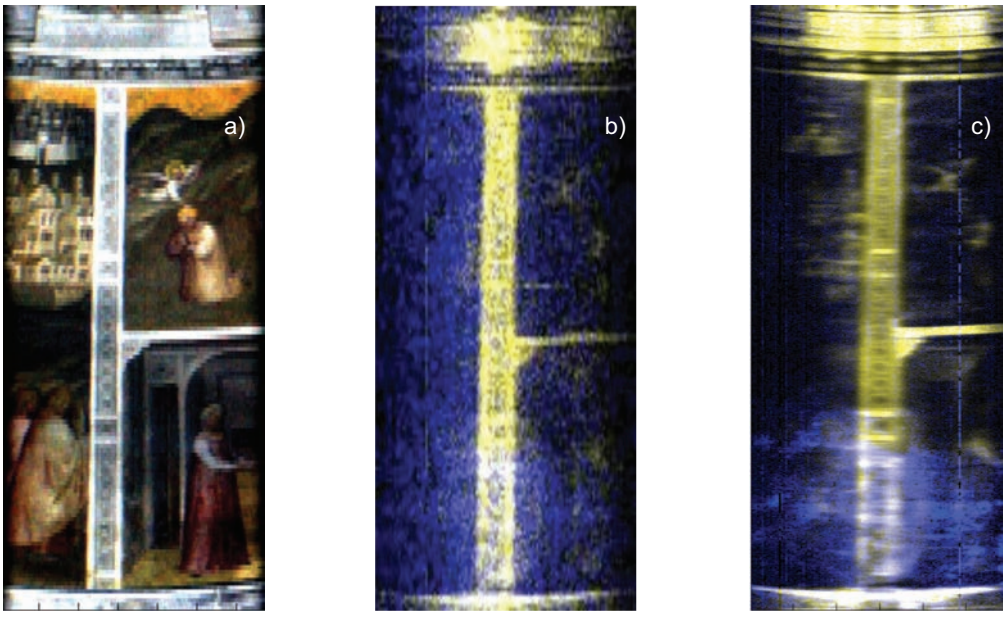

Figure 23 – Band analysis of scan T20 to T22: a) RGB colour image from spectrocolorimetric data; b) false colour reconstruction (RG420, B293); c) false colour reconstruction (RG480, B370).

By suitable image processing it is possible to emphasize the area with the highest content of superficial consolidant as shown in Figure 24. In Figure 24a we report, for the sake of comparison, the same image of Figure 23c, while in the right part we report a colour enhanced version of the very same fluorimetric data; by adopting this procedure it is possible to put in well evidence treated or consolidated areas.

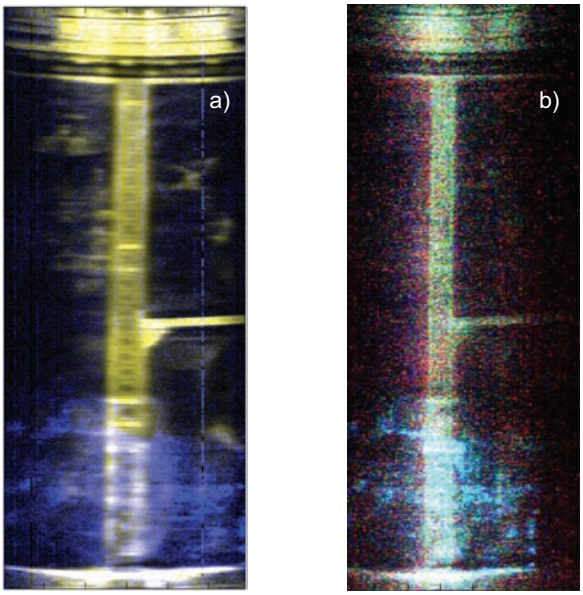

Figure 24 – Band analysis of scan T20: a) false colour reconstruction (RG420, B293); b) grey level scale of the intensity at F375 band with background at 354 nm and 390 nm.

3.4 Scan in the tambour with λ_{ex}=355 nm

Two regions in the *tambour* were scanned by the LIF apparatus with excitation at 355 nm in order to detect depigmentation, biological attack and salt effluorescence. The LIF system was placed at about 1.5 m distance from the target and the images acquired by point by point scanning approach with a spatial resolution of approximately 0.008 m. Typical scan sizes were 140 pixels width and 100 to 140 pixels height. More than 220 spectral channels were acquired from 300 nm to 870 nm. The details of the acquisition mode for the scans acquired on *tambour* are summarized in Tables 13 and 14.

Identification of bands in LIF spectra

The identification of band in LIF spectra was preceded by a PC analysis. Figure 25 shows the PC components of images A1 (fig. 25a) and of A2 (fig. 25b). The comparison of the two PCs shown in Figure 25 reveals differences in the spectral amplitude around the 350-390 nm region. The most interesting spectral features observed in Figure 25 are:

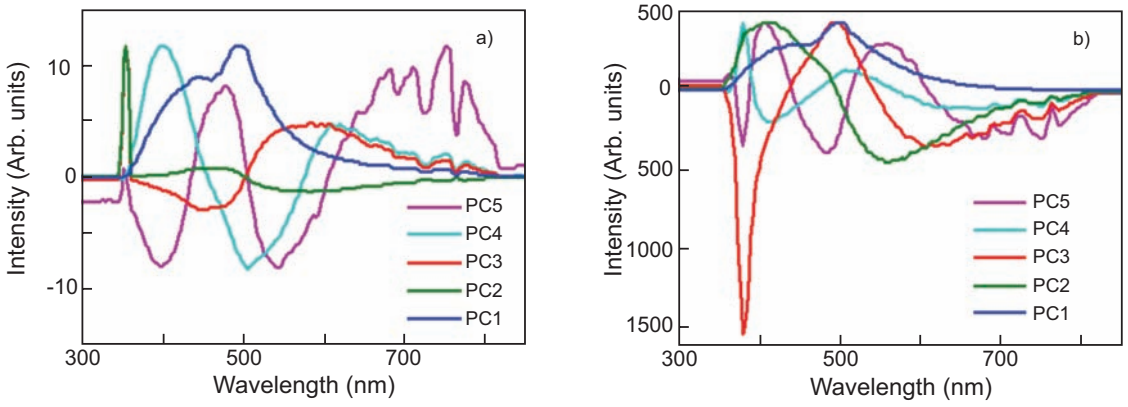

Figure 25 – PC analysis of LIF scans A1 a), and A2 b).

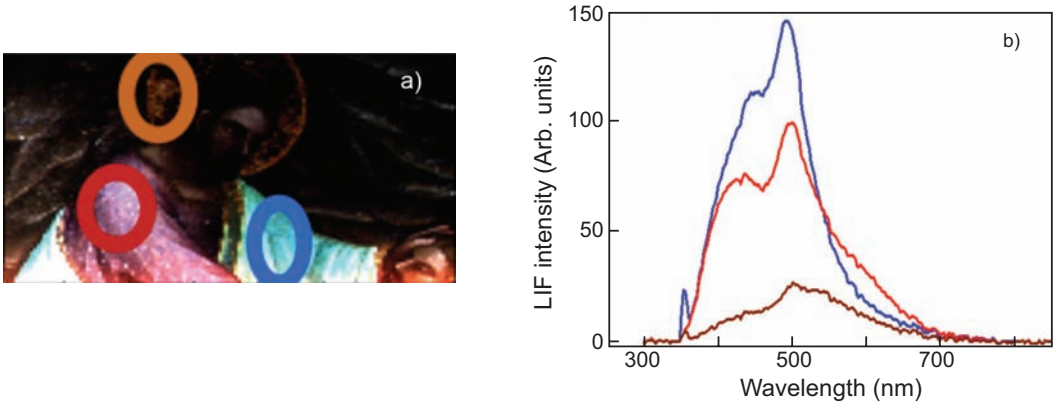

Figure 26 – Band analysis of scan A1: a) false colour reconstruction (R600, G500, B380); b) LIF spectra of selected areas.

- the elastic backscatter at 355 nm is visible only in A1 scan;
- narrowband emission with a peak at 380 nm (FWHM 15 nm) appear in A2 scan;
- broadband emission in the region 400-550 nm

While the emission at 355 nm is certainly attributed to the elastic scattering of the exciting laser light, the chemical substance responsible for the high emission at 380 nm is not definitively assigned. Our analysis will then proceed first by looking to their occurrence in the acquired scans, successively an interpretation is attempted based on comparison with a reference spectral data base.

Figure 26 shows the RGB false color reconstruction of scan A1; it is worth noticing here the closer similarity to the conventional color photograph, while a striking difference is evidenced by comparing this figure with Figure 18 (RGB false color image with excitation at 266 nm). One possible explanation can be found because the fluorescence induced by 355 nm from underneath plaster is whitish and its emission is modulated by the layered pigments. Significant differences are appreciated by observing the LIF spectra induced by different excitation wavelengths in the same areas; by comparing Figures 18 and Figure 26 we see a spectral shift towards longer wavelength: this is the case for the prominent emission at 420 nm now shifted to 500 nm; the red pigment still has a bimodal spectrum with relative maxima at 420 nm and 510 nm. The high emission peaked at 510 nm is here attributed to plaster emission, eventually emerging in depigmented areas (see images acquired in Hrastovlje church).

An interesting feature of scan A1 is presented in Figure 27, showing the false color representation obtained combining the elastic backscattered channel at 355 nm in the blue channel, with the emission at 500 nm in the green and red channels. A prominent elastic emission is here evidenced in two blue colored spots: to understand this experimental finding we examine the spectral content of fluorescence induced by 266 nm excitation on the very same portion of frescoed wall (it is marked in Figure 18 by the heavy blue spot and the corresponding spectrum). Fluorescence induced by the deeper UV excitation has emissions peaked at 293 nm, 310 nm and 370 nm suggesting the presence of PARALOID and other chemicals; however no spatial inhomogeneity is appreciated on the scanned surface. We conclude that the areas with high reflectance at 355 nm are those in which the exciting laser radiation was by chance close to normal incidence, having a reflection several orders of magnitude higher than in not normal direction; this explanation is also consistent with the smooth edges of the high reflectance areas.

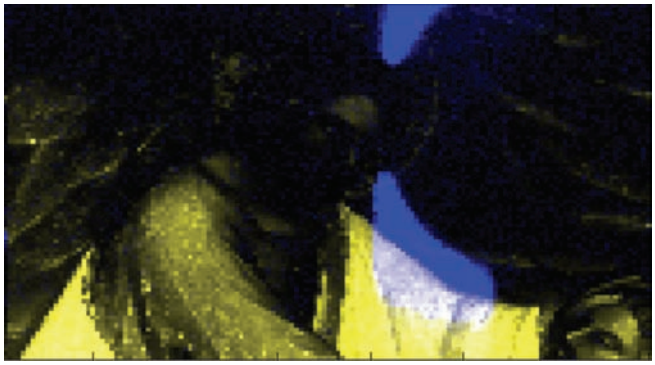

Figure 27 – RGB false colour reconstruction of A1 with near zero reflection of the excitation wavelength at 355nm (evidenced by blue spots).

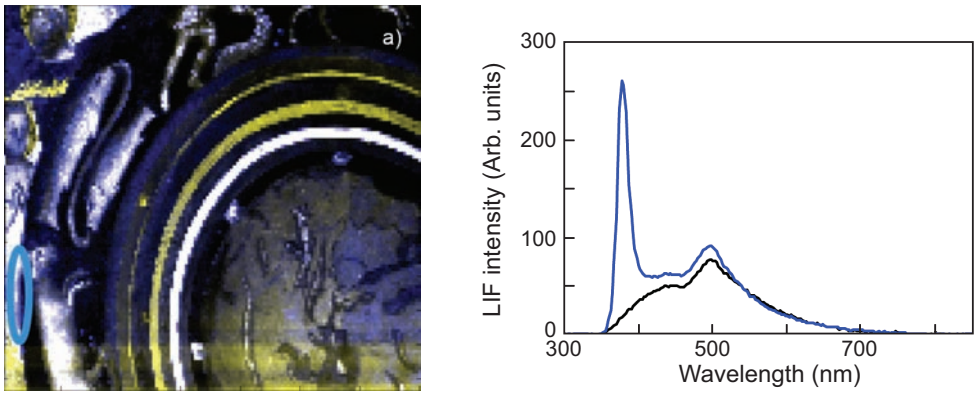

Figure 28 – Band analysis of scan A2: a) false colour reconstruction (RG600, B380); b) LIF spectrum of the selected area (blue line) and image averaged spectrum (black line).

Figure 28a shows the false colour RGB reconstruction from fluorescence data of scan A2, while spectra on selected areas are reported in Figure 28b. Following the suggestion gained by PCA, we are looking for large areas with strong emission at 380 nm, however this in not observed and only a very limited number of pixels have the strong emission bands peaked at 380 nm. While this emission is certainly due to the presence of a superficial layer, its assignments to a specific substance at this moment cannot be definitive. As final comment we notice how the excitation at 355 nm is able to induce fluorescence of consolidants only if present at very high concentrations.

4. Conclusions

The main results of the image analysis here presented can be summarized as follows:

- the ENEA LIF hyper spectral scanning system proved its ability to remotely and non invasively investigate large areas of painted surfaces with a multilayered structure;
- images can be quickly collected and released in false colors based on most prominent spectral features;
- high resolution distributions of materials with well characterized spectral features have been recorded, their assignment to different pigments and consolidants is still preliminary, due to the limited data bases available;

- additional in situ measurements are suggested to definitely discard some possible assignment of Raman bands;
- the precise localization of anomalous areas with presence / absence of specific pigments and consolidant is suitable to address further *in situ* measurements;
- statistical analysis and projections operators demonstrated their ability to automatic and semi automatic data processing in order to rebuild false colour images with prominent features stressing information useful to the restores.

References

1. F. Colao, R. Fantoni, L. Fiorani, A. Palucci, "*Dispositivo portatile a fluorescenza per la scansione spaziale di superfici, in particolare nell'ambito dei beni culturali*" Patent RM2007A000278 (2007).

2. L. Caneve, F. Colao, L. Fiorani, A. Palucci, "*Radar laser portatile per la diagnostica remota di superfici*" Patent RM2010A000606 (2010).

3. J. Striber, F. Colao, R. Fantoni, L. Fiorani, A. Palucci, *"Algorithm for angular correction of images in scanning LI"*, *J. Optoelectr. Adv. Mater.* **9**, 1918-1925 (2007).

4. F. Colao, R. Fantoni, L. Fiorani, A. Palucci, I. Gomoiu, *"Compact scanning lidar fluorosensor for investigations of biodegradation on ancient painted surfaces"*, *J. Optoelectr. Adv. Mater.* **7**, 3197–3208 (2005).

5. M.T. Doménech-Carbó, A. Doménech-Carbó, J.V. Gimeno-Adelantado, F. Bosch-Reig, "*Identification of synthetic resins used in works of art by fourier transform infrared spectroscopy", Appl. Spectros* **55**, 1590-1602 (2001).

6. L. Caneve, F. Colao, R. Fantoni, L. Fornarini, *"Laser induced fluorescence analysis of acrylic resins used in conservation of cultural heritage"*, Proceedings of OSAV'2008, The 2nd Int. Topical Meeting on Optical Sensing and Artificial Vision, St. Petersburg, Russia, (2008) pp. 57- 63.

7. F. Colao, L. Caneve, A. Palucci, R. Fantoni, L.Fiorani, *"Scanning hyperspectral lidar fluorosensor for fresco diagnostics in laboratory and field campaigns",* Lasers in the Conservation of Artworks (LACONA VII), Eds. J. Ruiz, R. Radvan, M. Oujja, M. Castillejo, P. Moreno, CRC Press, 149–155, (2008).

8. I. Borgia, R. Fantoni, C. Flamini, T.M. Di Palma, A. Giardini Guidoni, A. Mele, *"Luminescence from pigments and resins for oil paintings induced by laser excitation"*, Vol. **127-129**, pp. 95-100 (1998).

9. D. Anglos, M. Solomidou, I. Zergioti, V. Zaffiropulos, T.G. Papazoglou, C. Fotakis, *"Laser-induced fluorescence in artwork diagnostics: an application in pigment analysis"*, Appl. Spectrosc. **50**, (1996) pp. 1331-1334.

Appendix

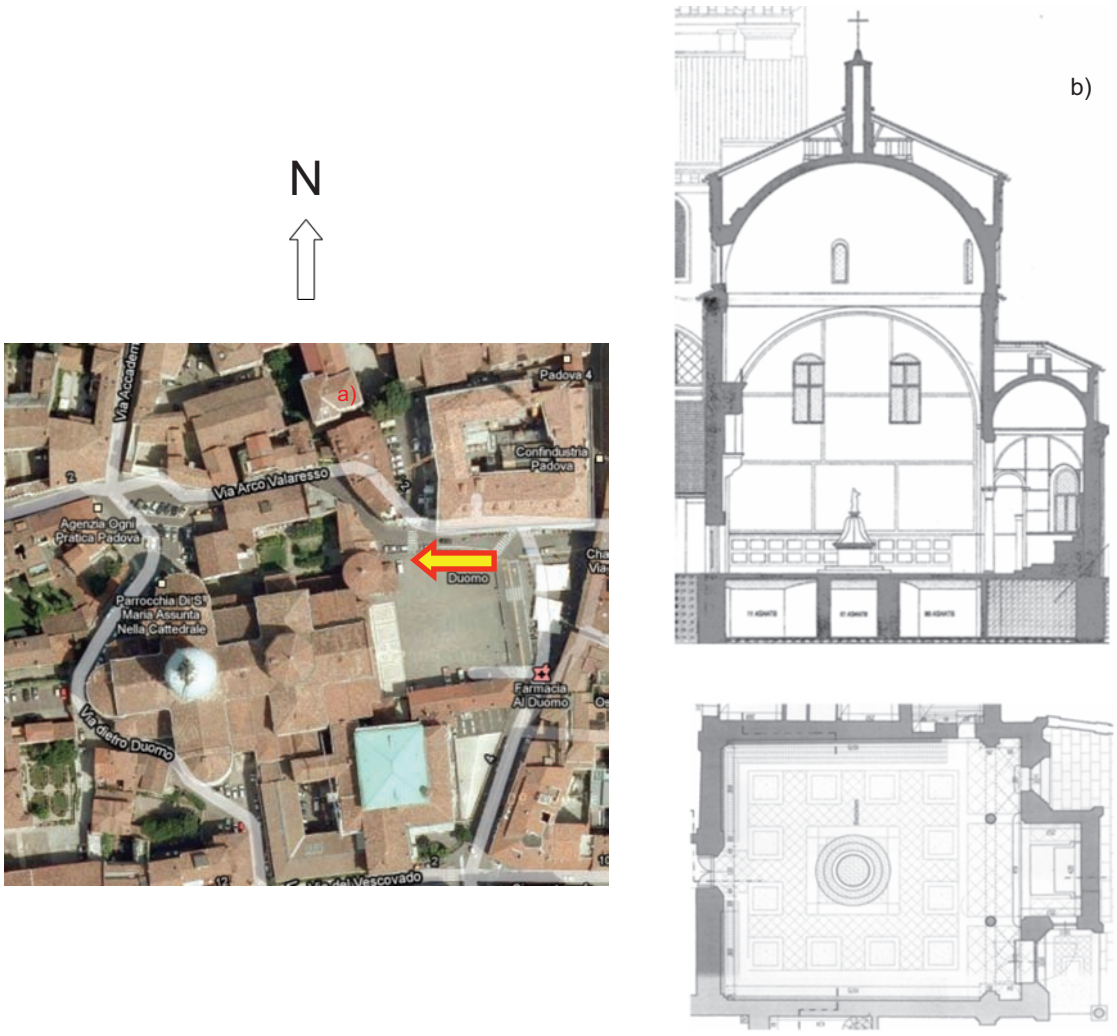

Figure A1 – a) Location and b) drawing of Padua Baptistery.

Edito dall' ENEA
Servizio Comunicazione

Lungotevere Thaon di Revel, 76 - 00196 Roma

www.enea.it

Stampa: Tecnografico ENEA - CR Frascati
Pervenuto il 7.5.2012
Finito di stampare nel mese di maggio 2012